

Selected topics on parton distribution functions

M. Hirai*, H. Kawamura[†], S. Kumano^{†,**} and K. Saito*

**Department of Physics, Faculty of Science and Technology, Tokyo University of Science
2641, Yamazaki, Noda, Chiba, 278-8510, Japan*

[†]*KEK Theory Center, Institute of Particle and Nuclear Studies, KEK
1-1, Oho, Tsukuba, Ibaraki, 305-0801, Japan*

***J-PARC Branch, KEK Theory Center, Institute of Particle and Nuclear Studies, KEK
and Theory Group, Particle and Nuclear Physics Division, J-PARC Center
203-1, Shirakata, Tokai, Ibaraki, 319-1106, Japan*

Abstract. We report recent studies on structure functions of the nucleon and nuclei. First, clustering effects are investigated in the structure function F_2 of ${}^9\text{Be}$ for explaining an unusual nuclear correction found in a JLab experiment. We propose that high densities created by formation of clustering structure like 2α +neutron in ${}^9\text{Be}$ is the origin of the unexpected JLab result by using the antisymmetrized molecular dynamics (AMD). There is an approved proposal at JLab to investigate the structure functions of light nuclei including the cluster structure, so that much details will become clear in a few years. Second, tensor-polarized quark and antiquark distributions are obtained by analyzing HERMES measurements on the structure function b_1 for the deuteron. The result suggests a finite tensor polarization for antiquark distributions, which is an interesting topic for further theoretical and experimental investigations. An experimental proposal exists at JLab for measuring b_1 of the deuteron as a new tensor-structure study in 2010's. Furthermore, the antiquark tensor polarization could be measured by polarized deuteron Drell-Yan processes at hadron facilities such as J-PARC and GSI-FAIR. Third, the recent CDF dijet anomaly is investigated within the standard model by considering possible modifications of the strange-quark distribution. We find that the shape of a dijet-mass spectrum changes depending on the strange-quark distribution. It indicates that the CDF excess could be partially explained as a PDF effect, particularly by the strangeness in the nucleon, within the standard model if the excess at $m_{jj} \approx 140$ GeV is not a sharp peak.

Keywords: Quark, gluon, parton, distribution, QCD, nuclear effect, tensor, jet, CDF anomaly

PACS: 13.60.Hb, 13.60.-r, 24.85.+p, 13.88.+e, 13.87.-a

INTRODUCTION

Studies of parton distribution functions (PDFs) are important for investigating internal structure of hadrons and for calculating precise cross sections in hadron reactions. The precise information is necessary for finding any new physics beyond the standard model and new phenomena in hadron and nuclear physics. Recently, there are interesting findings and progresses on high-energy hadron reactions. We explain the following selected topics in this report:

1. a possible clustering effect in the structure function F_2 of the ${}^9\text{Be}$ nucleus [1, 2],
2. tensor structure in quark and gluon degrees of freedom by the structure function b_1 [3, 4],
3. test of CDF dijet anomaly within the standard model [5, 6].

We explain these topics by the following sections.

NUCLEAR CLUSTERING EFFECTS

Nuclear modifications of the structure function F_2 were recently measured at the Thomas Jefferson National Accelerator Facility (JLab) for light nuclei. By taking the x -slope of the ratio F_2^A/F_2^D , namely $|d(F_2^A/F_2^D)/dx|$, they observed an anomalously large nuclear effect in ${}^9\text{Be}$ as shown in Fig.1. It is too large to be expected from an average nuclear density.

It is known that clustering structure is expected to exist for light nuclei around the mass number $A = 10$ according to theoretical nuclear models such as antisymmetrized (or fermionic) molecular dynamics (AMD or FMD). We consider that an anomalous nuclear modification of the ${}^9\text{Be}$ structure function could be related to the nuclear cluster structure. We investigated a possible clustering effect by using the AMD and shell-model wave functions for the ${}^9\text{Be}$ nucleus. We show a possibility to explain the anomalous JLab result by cluster formation [2].

Nuclear structure functions are described by a convolution picture [7, 8]:

$$F_2^A(x, Q^2) = \int_x^A dy f(y) F_2^N(x/y, Q^2), \quad f(y) = \frac{1}{A} \int d^3 p_N y \delta\left(y - \frac{p_N \cdot q}{M_N v}\right) |\phi(\vec{p}_N)|^2, \quad (1)$$

where y is the momentum fraction $y = M_A p_N \cdot q / (M_N p_A \cdot q)$. The nucleon momentum distribution $\phi(\vec{p}_N)$ is calculated in two models. One is the simple shell model, and the other is the AMD in order to illustrate clustering effects by differences between the two-model results. An advantage of the AMD is that there is no assumption on nuclear structure, namely shell or cluster-like configuration. The spacial density distributions are shown in Fig.2 for ${}^4\text{He}$ and Fig.3 for ${}^9\text{Be}$. The density distributions are the same in both shell-model and AMD for ${}^4\text{He}$. However, the AMD density of ${}^9\text{Be}$ in Fig.3 is much different from a monotonic shell-model density similar to the one in Fig.2. It is obvious that ${}^9\text{Be}$ has two α clusters with neutron clouds.

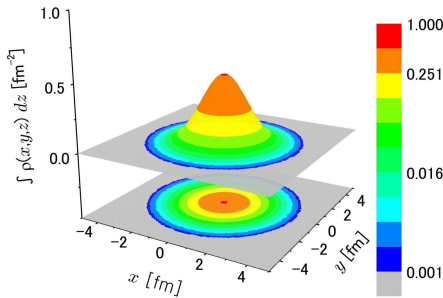


FIGURE 2. Density distribution of ${}^4\text{He}$ [2].

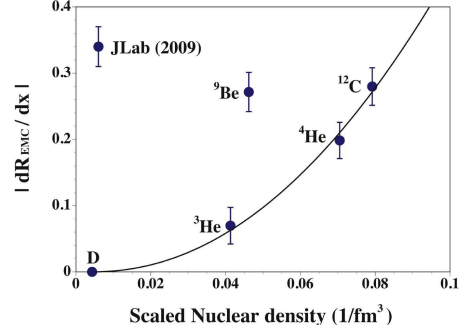


FIGURE 1. Nuclear modifications $|d(F_2^A/F_2^D)/dx|$ for light nuclei.

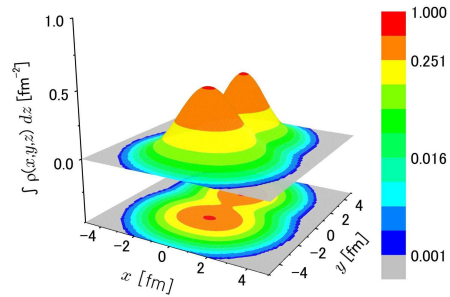


FIGURE 3. Density distribution of ${}^9\text{Be}$ by AMD [2].

Calculated nuclear modifications are shown in Fig.4. Although the nuclear density distributions are much different in the shell and AMD models, the clustering effects, namely the differences between the solid and dashed curves, are not very large in Fig.4 due to angular average in calculating the convolution integral. The theoretical curves do not agree quite well with the experimental data, which is partly because short-range-correlation effects are not taken into account in the nucleon momentum distribution and the separation energy. The small difference between the shell and AMD results suggests that the mean conventional mechanism does not solve the anomalously large nuclear modification.

Next, we consider that the high-densities created by the formation of clusters in Fig. 3 could be the origin of the large JLab modification. Obviously, the density peaks in the two clusters are much larger than shell-model densities. We calculated maximum local densities in both shell and AMD models. The JLab data are shown by the calculated maximum local densities in Fig.5. The curve is the interpolation of shell-model data points except for ${}^9\text{Be}$. If the ${}^9\text{Be}$ data point is shown by the density of the shell model, it significantly deviates from the curve. However, if it is plotted by the AMD density, it agrees with the curve. This fact suggests that *the JLab result should be caused by the high densities created by the cluster formation in ${}^9\text{Be}$* [2].

We consider that the nuclear structure functions consist of the mean conventional part and the remaining one depending on the maximum local density:

$$F_2^A = (\text{mean part}) + (\text{part created by large densities due to cluster formation}). \quad (2)$$

The first part is calculated by the convolution integral of Eq.(1) and the second part seems to play a crucial role in explaining the JLab anomaly. The physics mechanism for the second term is likely to be the modification of internal nucleon structure caused by the cluster formation.

Our studies in Ref. [2] stimulated JLab experimentalists to investigate possible cluster structure in an approved experimental proposal to measure the structure functions of light nuclei [9] including ${}^6\text{Li}$, ${}^7\text{Li}$, ${}^{10}\text{B}$, and ${}^{11}\text{B}$ in addition to ${}^9\text{Be}$. Therefore, much details should become clear in a few years by precise JLab measurements after 12 GeV upgrade.

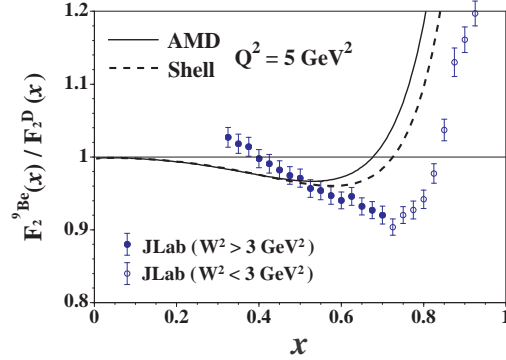


FIGURE 4. F_2^{9Be}/F_2^D by shell and AMD models [2].

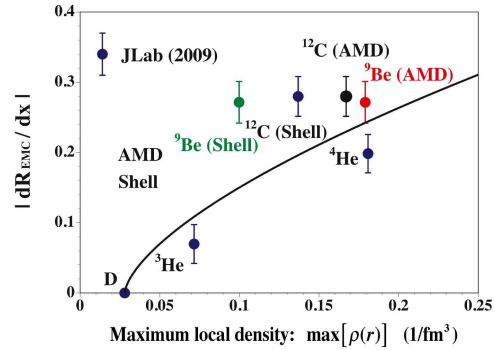


FIGURE 5. Nuclear modification slopes shown by maximum local densities [2].

TENSOR STRUCTURE FUNCTION

Tensor structure of the deuteron has been investigated for a long time by hadron degrees of freedom as explained in standard nuclear-physics textbooks. However, the time has come to describe it in terms of quark and gluon degrees of freedom. In particular, the first measurement of the tensor structure function b_1 has been reported by the HERMES collaboration [3]. As illustrated in Fig.6, b_1 vanishes if constituents are in the S -wave. In the “standard model” of the deuteron with D -state admixture, a finite b_1 is obtained, for example, in the convolution picture for the structure function. If experimental measurements are different from this standard-model predication, it should provide opportunities for interesting new aspects in the tensor structure.

Tensor structure b_1 for deuteron

Tensor-structure crisis!?

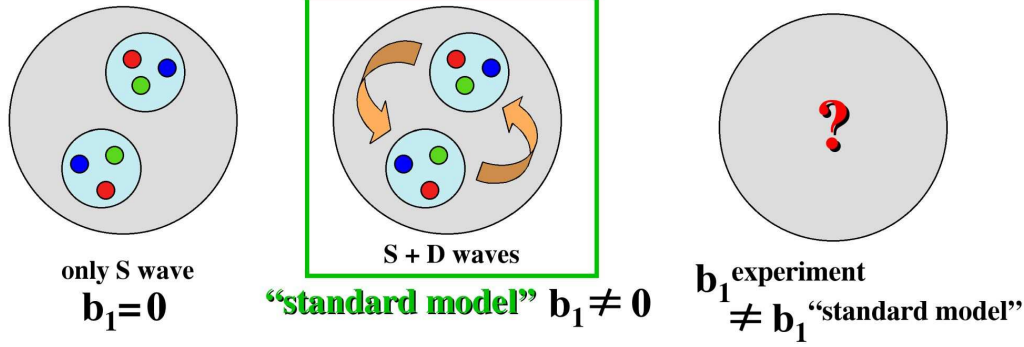


FIGURE 6. Illustration of tensor structure in the deuteron.

In this work, tensor polarized quark and antiquark distribution functions are extracted from the HERMES measurement. The b_1 is expressed by tensor-polarized distributions $\delta_T q$ as

$$b_1(x) = \frac{1}{2} \sum_i e_i^2 [\delta_T q_i(x) + \delta_T \bar{q}_i(x)], \quad \delta_T q_i(x) = q_i^0(x) - \frac{q_i^{+1}(x) + q_i^{-1}(x)}{2}, \quad (3)$$

where q_i^λ indicates an unpolarized-quark distribution in the hadron spin state λ . In analyzing b_1 data, the distributions $\delta_T q$ and $\delta_T \bar{q}$ are parametrized as [4]

$$\delta_T q_{iv}^D(x) = \delta_T w(x) q_{iv}^D(x), \quad \delta_T \bar{q}_i^D(x) = \alpha_{\bar{q}} \delta_T w(x) \bar{q}_i^D(x), \quad \delta_T w(x) = ax^b(1-x)^c(x_0-x), \quad (4)$$

by considering that certain fractions of unpolarized distributions are tensor polarized. Here, flavor-symmetric antiquark distribution [10] are assumed for tensor polarization. The parameters $\alpha_{\bar{q}}$, a , b , and c are determined by analyzing the HERMES data with the following two options:

- Set 1: Tensor-polarized antiquark distributions are terminated ($\alpha_{\bar{q}} = 0$).
- Set 2: Finite tensor-polarized antiquark distributions are allowed ($\alpha_{\bar{q}}$ is a parameter).

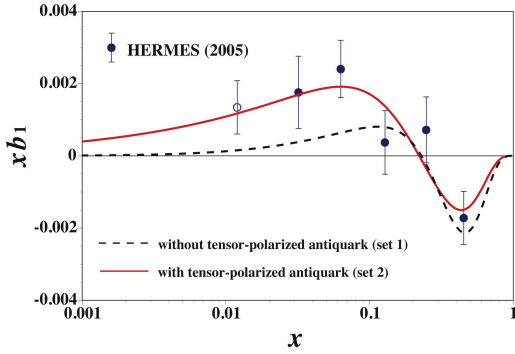


FIGURE 7. Two analysis results are shown with the HERMES b_1 data [4].

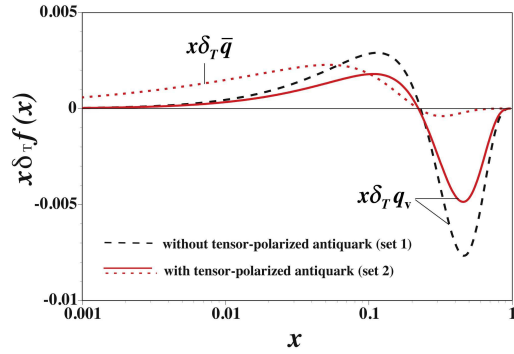


FIGURE 8. Obtained tensor-polarized distributions [4].

Analysis results are shown with the HERMES data in Fig.7. The dashed curve without the antiquark polarization does not agree with the data in the small- x region; however, the solid curve of the set-2 analysis agrees well with the data. Obtained tensor-polarized quark and antiquark distributions are shown in Fig.8. It is interesting to find a finite tensor-polarized antiquark distributions. It was shown in Ref. [11] that the first moment of b_1 is related to a finite tensor polarization of antiquarks in Eq. (5):

$$\int dx b_1(x) = -\frac{5}{24} \lim_{t \rightarrow 0} t F_Q(t) + \frac{1}{18} \int dx [8\delta_T \bar{u}(x) + 2\delta_T \bar{d}(x) + \delta_T s(x) + \delta_T \bar{s}(x)], \quad (5)$$

$$\int \frac{dx}{x} [F_2^p(x) - F_2^n(x)] = \frac{1}{3} + \frac{2}{3} \int dx [\bar{u}(x) - \bar{d}(x)], \quad (6)$$

where $F_Q(t)$ is the quadrupole form factor. This b_1 sum rule is very similar to the Gottfried sum, which indicates a finite $\bar{u} - \bar{d}$ by the deviation from $1/3$ in Eq. (6). In the analysis of set-2, the sum is $\int dx b_1(x) = 0.0058$ [4]. According to Eq. (5), it should be related to a finite antiquark tensor polarization, which is interesting for further theoretical investigations on a possible mechanisms to create it.

In Fig.7, it is obvious that much better measurements are needed to investigate more details. Because there is a proposal to measure b_1 at JLab [12], much details of the tensor structure will be investigated in a few years. On the other hand, an appropriate future experiment to probe the antiquark tensor polarization is a Drell-Yan experiment, for example, by proton-deuteron Drell-Yan with a polarized deuteron target [13]. It could be possible at hadron facilities such as J-PARC (Japan Proton Accelerator Research Complex) [14] and GSI-FAIR (Gesellschaft für Schwerionenforschung -Facility for Antiproton and Ion Research). Hadron-tensor studies become a new era in terms of quark and gluon degrees of freedom!

CDF DIJET ANOMALY WITHIN STANDARD MODEL

The CDF anomaly [5] was observed in the dijet-mass distribution in $p\bar{p}$ collisions by observing events with two energetic jets, one high- p_T electron or muon, and missing E_T . However, another experimental group *D0* did not observe the same phenomenon [15]. Here, we investigate a possibility to explain it within the standard model as effects of the PDFs. A fraction of the proton or antiproton beam energy 980 GeV (=1.96 TeV /2) needs to be transferred to one of the dijets with the energy about 70 GeV (=140 GeV /2), so that PDFs of the $x = 0.1$ region affect the CDF result. Since light-quark (u and d) distributions are well determined at $x \sim 0.1$, we focus our attention to the strange-quark distribution $s(x)$. In particular, the Bjorken variable- x dependence of $s(x)$ is not known. The 2nd moment of $s(x)$ is determined by the neutrino-induced dimuon measurements in comparison with the 2nd moment of the light-antiquark distributions. Then, a similar or same x -dependent functional form is assumed for $s(x)$ as $[\bar{u}(x) + \bar{d}(x)]/2$. It is typically illustrated by the HERMES experiment [16], which indicates a much softer $s(x)$ distribution as shown in Fig.9. The CDF dijet anomaly could be related to such an issue of the strange-quark distribution.

The strange-quark distribution is roughly 40% of the light antiquark distribution $[\bar{u}(x) + \bar{d}(x)]/2$ as shown by the solid curve in Fig.9. However, recent HERMES experiment indicated the much softer distribution as it becomes close to $x(\bar{u} + \bar{d})$ at small x and it almost vanishes at $x > 0.1$. The HERMES measurement was done by semi-inclusive kaon production in charged-lepton deep inelastic scattering. It should be noticed that kaon fragmentation functions have large uncertainties as typically shown in Ref. [18], so that the HERMES determination of $s(x)$ may not be accurate. Therefore, we take a hard strange-quark distribution shown by the dot-dashed curve as one of trial functions in estimating PDF effect on the dijet cross section in addition to the CTEQ6L1 and HERMES-like soft distribution. Like the intrinsic charm distribution at large x [19], there could be intrinsic strange distribution [10, 20] which gives rise to the excess of $s(x)$ at large x . The average scale of the HERMES experiment is $Q^2 = 2.5 \text{ GeV}^2$, so that the distributions should be evolved to a hard scale in the CDF experiment. The

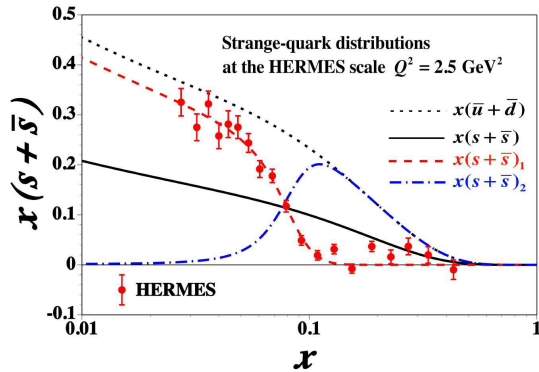


FIGURE 9. Strange-quark distribution by HERMES [16], CTEQ6L1 distribution [17], and a possible hard strange-quark distribution [6].

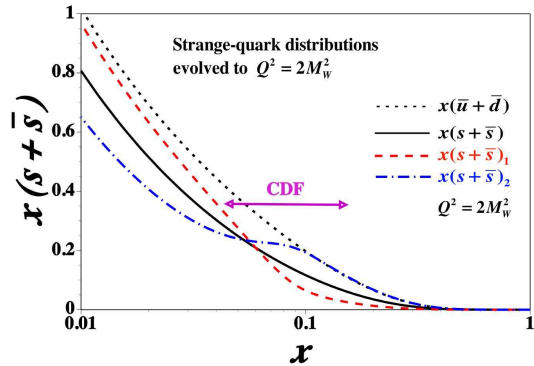


FIGURE 10. The strange-quark distributions in Fig.9 are evolved to the scale $Q^2 = 2M_W^2$ in the CDF experiment [6].

strange-quark distributions $s + \bar{s}$, $(s + \bar{s})_1$, and $(s + \bar{s})_2$ in Fig.9 are evolved to the typical hard scale $Q^2 = 2M_W^2$ in the CDF dijet measurement by the Q^2 evolution code of Ref. [21]. The evolved distributions are shown in Fig.10 together with $x(\bar{u} + \bar{d})$ at $Q^2 = 2M_W^2$. If the distributions are evolved to such a large scale, the differences between the three distributions are not as large as the ones in Fig.9 because strange quarks are copiously produced by the Q^2 evolution.

There are various processes which contribute to the dijet events. We calculated the processes W +dijet, Z +dijet, top, WW , and WZ by the event generator GR@PPA (GRace At Proton-Proton/Antiproton collisions) [22]. By supplying kinematical conditions and a reaction process, the GR@PPA automatically calculates possible processes and their contributions to a cross section. Effects of $s(x)$ on the dijet cross section are shown in Fig.11. In our work, the partonic cross sections are calculated, and subsequent parton shower and final fragmentations into hadrons are not included. They

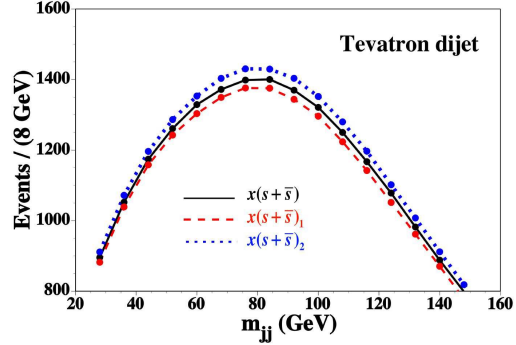


FIGURE 11. Effects of $s(x)$ on dijet events [6].

could be calculated, for example, by using the event generator PYTHIA. It is the purpose of this work to show gross properties of strange-quark effects simply by calculating the hard process part. Furthermore, since the detector acceptance information is not available for public, the overall magnitude of the events cannot be compared with the CDF measurements. We may look at overall shapes of the events.

According to the results in Fig.11, the dijet-mass distribution increases if the hard distribution $(s + \bar{s})_2$ is taken, whereas it decreases for the soft one $(s + \bar{s})_1$. We also notice the shape of the dijet-mass distribution changes depending on the strange-quark distribution. Since the CDF anomaly was observed in the shoulder region of $m_{jj} \approx 140$ GeV, a slight change of the dijet-mass distribution could explain at least partially the anomalous excess if it is not a strong peak [6]. We also calculated effects of the strange-quark modifications on the dijet cross section at LHC. We found sizable effects in the LHC kinematics; however, the results are sensitive to a different x region ($x \sim 0.02$) because of the larger center-of-mass energy of 14 TeV. Therefore, the x dependence of the strange-quark distribution should be constrained by future LHC measurements together with Tevatron data.

In our studies, the possible variations of $s(x)$ are investigated and their effects on the CDF dijet cross sections are calculated. We found that the effects are sizable in W +dijet and Z +dijet processes and that they are very small in other processes (top, WW , WZ). It is important to consider such PDF effects within the standard model for testing whether the CDF anomaly actually indicates new physics beyond the standard model. Further theoretical and experimental investigations are needed including physics mechanisms of creating the strange-quark distribution other than the one produced by the obvious Q^2 evolution.

ACKNOWLEDGEMENTS

This work was partially supported by a Grant-in-Aid for Scientific Research on Priority Areas "Elucidation of New Hadrons with a Variety of Flavors (E01: 21105006)" from the ministry of Education, Culture, Sports, Science and Technology of Japan.

REFERENCES

1. J. Seely *et al.*, Phys. Rev. Lett. **103**, 202301 (2009).
2. M. Hirai, S. Kumano, K. Saito, and T. Watanabe, Phys. Rev. C **83**, 035202 (2011).
3. A. Airapetian *et al.* (HERMES Collaboration), Phys. Rev. Lett. **95**, 242001 (2005).
4. S. Kumano, Phys. Rev. D **82**, 017501 (2010).
5. T. Aaltonen *et al.* (CDF Collaboration), Phys. Rev. Lett. **106**, 171801 (2011).
6. H. Kawamura, S. Kumano, and Y. Kurihara, KEK-TH-1493 (J-PARC-TH-0001), arXiv: 1110.6243 [hep-ph].
7. D. F. Geesaman, K. Saito, and A. W. Thomas, Ann. Rev. Nucl. Part. Sci. **45**, 337 (1995).
8. M. Ericson and S. Kumano, Phys. Rev. C **67**, 022201 (2003).
9. Jefferson Lab PAC-35 proposal, PR12-10-008, J. Arrington *et al.* (2009).
10. S. Kumano, Phys. Rept. **303**, 183 (1998); G. T. Garvey and J.-C. Peng, Prog. Part. Nucl. Phys. **47**, 203 (2001).
11. F. E. Close and S. Kumano, Phys. Rev. D **42**, 2377 (1990).
12. Jefferson Lab PAC-38 proposal, PR12-11-110, J.-P. Chen, P. Solvignon, N. Kalantarians, O. Rondon, K. Slifer *et al.* (2011).
13. S. Hino and S. Kumano, Phys. Rev. D **59**, 094026 (1999); **60**, 054018 (1999); S. Kumano and M. Miyama, Phys. Lett. B **479**, 149 (2000).
14. See <http://j-parc.jp/index-e.html>. S. Kumano, Nucl. Phys. A **782**, 442 (2007); AIP Conf. Proc. **1056**, 444 (2008); J. Phys. Conf. Ser. **312**, 032005 (2011).
15. V. M. Abazov *et al.* (D0 Collaboration), Phys. Rev. Lett. **107**, 011804 (2011).
16. A. Airapetian *et al.* (HERMES Collaboration), Phys. Lett. B **666**, 446 (2008).
17. J. Pumplin *et al.* (CTEQ Collaboration), JHEP **07**, 012 (2002).
18. M. Hirai, S. Kumano, T.-H. Nagai, and K. Sudoh, Phys. Rev. D **75**, 094009 (2007).
19. S. J. Brodsky, P. Hoyer, C. Peterson, and N. Sakai, Phys. Lett. B **93**, 451 (1980); J. Pumplin, H. L. Lai, and W. K. Tung, Phys. Rev. D **75**, 054029 (2007).
20. S. J. Brodsky and B.-Q. Ma, Phys. Lett. B **381**, 317 (1996); H. Chen, F.-G. Cao, and A. I. Signal, J. Phys. G **37**, 105006 (2010) and references therein.
21. M. Miyama and S. Kumano, Comput. Phys. Commun. **94**, 185 (1996).
22. S. Odaka and Y. Kurihara, arXiv:1107.4467 [hep-ph]; S. Tsuno, T. Kaneko, Y. Kurihara, S. Odaka, and K. Kato, Comput. Phys. Commun. **175**, 665 (2006).